

## Breath figure pattern formation as a means to fabricate micro-structured organic light-emitting diodes

This article has been downloaded from IOPscience. Please scroll down to see the full text article.

2007 J. Phys.: Condens. Matter 19 016203

(<http://iopscience.iop.org/0953-8984/19/1/016203>)

View [the table of contents for this issue](#), or go to the [journal homepage](#) for more

Download details:

IP Address: 129.252.86.83

The article was downloaded on 28/05/2010 at 15:03

Please note that [terms and conditions apply](#).

# Breath figure pattern formation as a means to fabricate micro-structured organic light-emitting diodes

M Pintani, J Huang, M C Ramon and D D C Bradley

Ultrafast Photonics Collaboration and Experimental Solid State Physics Group, The Blackett Laboratory, Imperial College London, Prince Consort Road, London SW7 2BZ, UK

E-mail: [D.Bradley@imperial.ac.uk](mailto:D.Bradley@imperial.ac.uk)

Received 5 August 2006, in final form 3 November 2006

Published 7 December 2006

Online at [stacks.iop.org/JPhysCM/19/016203](http://stacks.iop.org/JPhysCM/19/016203)

## Abstract

We demonstrate a procedure for fabricating micro-structured organic light-emitting diodes (micro-LEDs) based on so-called *breath figure* (BF) pattern formation. In the latter process water vapour is condensed on the surface of a spread polymer solution to form droplets that close pack into ordered arrays and that transfer the BF pattern into the resulting solid thin polymer film. Here, we generate a silicone elastomer negative replica of the BF pattern and use it as a master for solvent-assisted micro-moulding of an insulating polymer layer deposited on top of a PEDOT:PSS covered indium tin oxide (ITO)-coated glass substrate. By spin coating a light-emitting polymer blend film on top of the micro-structured insulator, we obtain micro-structured polymer LEDs with dimensions defined by the BF pattern.

## 1. Introduction

Breath figure (BF) pattern formation occurs when moist air comes into contact with a cold surface. First studies [1] concentrated on understanding how different substrate cleaning protocols, in particular heat or solvent exposure, influence the BF self-assembly process. Subsequently, growth laws were studied [2] for BF formation, with the initial hexagonal close-packed arrangement of water droplets being followed by a coalescence that gives rise to increasingly non-uniform patterns. More recently, Widawski *et al* [3] reported that BF patterns could be easily generated by flowing a stream of moist gas across the surface of a polymer solution spread on a glass substrate. In this case, solvent evaporation produces the cold surface needed for water vapour condensation, and the accompanying solidification of the polymer leads to the BF pattern being transferred into the resulting film. Such BF pattern formation in polymer films has attracted increasing interest over the last few years and the process offers exciting possibilities to create ordered two- (or even three-) dimensional hole-arrays using a simple one-step process. Moreover, the size of the holes can be tuned, typically in the range 0.2–20  $\mu\text{m}$  [4], by simply varying the parameters used in the formation

process, such as humidity, solvent, and polymer molecular weight [4, 5]. Such hole-arrays have potential for many applications, including membranes, picolitre beakers for synthesis or analysis, photonic crystal structures, and microlens arrays. However, it is only very recently that practical applications have started to be reported, for example membrane structures for cell growth studies [6] and templates for the fabrication of dichroic filters [7].

In this paper, we report the use of BF patterns in the micro-structuring of organic light-emitting diodes (LEDs), a process of interest for controlling light out-coupling [8–10] and for the fabrication of high-resolution displays [11–14]. Specifically, we prepare an elastomeric replica of a BF pattern and use this replica as the master with which to micro-contact print an insulating polymer layer on top of an indium tin oxide (ITO)-coated substrate. Spin coating a suitable conjugated polymer blend onto the patterned insulator and finally evaporating a metal cathode on top completes our micro-structured LEDs. Bolognesi *et al* [15] have recently reported similar studies, namely the use of a poly(dimethylsiloxane) (PDMS) replica to pattern a (conjugated) polymer film. These authors also suggested that micro-patterned LEDs could thus be made, but no information was provided on how this would be done, or on the resulting device performance.

The sub-micron potential for BF pattern formation [4] offers exciting prospects for the fabrication of structures in which optical confinement effects can be used to strongly control the spectral and spatial characteristics of emission within the near-infrared and visible ranges [16, 17]. However, even at much more modest length scales, namely microns, or even tens to hundreds of microns, there is interest in BF patterning. For instance, surface energy patterning for directed phase separation on micron length scales offers control over light out-coupling from polymer blend LEDs [18]. It has also been shown that LEDs with dimensions of tens to hundreds of microns can have significantly improved characteristics [11, 19] with better thermal management and improved device stability. Our earlier study [11] showed for example that an increase by a factor of nine in the current density was achievable on reducing the active area of a polyfluorene LED from a rectangle of  $1.5 \times 3 \text{ mm}^2$  to a  $50 \mu\text{m}$  diameter circle.

The procedure employed in this paper offers good prospects for low-cost fabrication since the master (subsequently used for printing) does not require a complicated subtractive patterning process to generate, contrary to the case of conventional optical lithography. Moreover, the solvent-assisted printing method that we use does not involve a direct patterning of the active polymer layer, and hence the possibility of degrading its emissive properties is avoided.

## 2. Fabrication of a micro-structured PDMS master

As the first step in our procedure, a few millilitres of a  $30 \text{ g l}^{-1}$  chloroform solution of the fluorene-arylene copolymer NFG were carefully spread on a microscope slide. Immediately thereafter, the solution-coated substrate was introduced into a sample chamber wherein moist nitrogen was flowed ( $2000 \text{ ml min}^{-1}$ ) across its surface. The moisture level was controlled by bubbling the nitrogen gas through a water bath on its way into the sample chamber. Water vapour condensation (droplet nucleation) was observed shortly after introduction: following nucleation, the water droplets grew and arranged themselves into a hexagonal close-packed array [4], the scattering from which rendered the solution film opaque. As the solvent continued to evaporate a solid polymer film was generated into which the BF pattern had clearly transferred. Figure 1(a) shows an atomic force microscope (AFM) image ( $25 \times 25 \mu\text{m}^2$ ) of such a structure with holes of  $\approx 2.5 \mu\text{m}$  diameter and 500–800 nm depth separated by polymer walls of  $\approx 1 \mu\text{m}$  thickness. The quasi-triangular shape observed is an AFM artefact, as could easily be shown using an optical microscope with which circular holes were evident. The pattern was found to be quite uniform over an area of a few square millimetres, although line defects

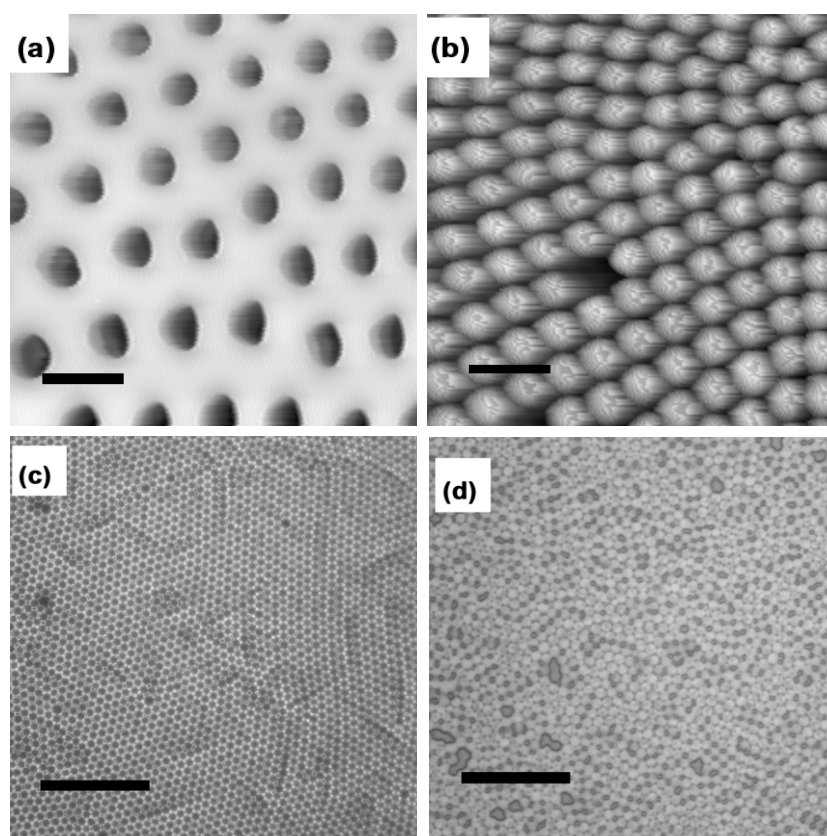


**Figure 1.** (a) An AFM image (Burleigh METRIS-2000) of a BF pattern formed in a polyfluorene copolymer film by exposure of a spread chloroform solution of the polymer to a moist nitrogen gas flow (the scale bar is  $5\ \mu\text{m}$ , maximum height  $0.8\ \mu\text{m}$ ). (b) An AFM image of a PDMS replica of such a BF pattern (the scale bar is  $5\ \mu\text{m}$ , maximum height  $1.1\ \mu\text{m}$ ). (c) An optical micrograph of a hole-array printed using the PDMS replica as a master for microcontact printing: the hole-array penetrates through a PI film deposited on top of a PEDOT layer spin coated onto an ITO-coated glass substrate (the scale bar is  $20\ \mu\text{m}$ ). (d) An optical micrograph of a PI patterned film (as per (c)) onto which an F8BT:TFB blend has been spin coated (the scale bar is  $20\ \mu\text{m}$ ).

(packing plane mismatches) and hole vacancies (missing holes) could be seen. In addition, the hole size changes slightly across the film ( $\pm 3\text{--}4\%$ ) due to differences in the evaporation rate at the edges and in the centre of the spread solution.

The patterned NFG film thus obtained was next employed to fabricate a silicone elastomer negative replica to use as a master for solvent-assisted micro-moulding. A Sylgard 184 (Dow Corning) poly(dimethylsiloxane) (PDMS) elastomer was used. It is supplied as a two-part kit containing a liquid silicone rubber precursor and a curing agent. The former is a vinyl-terminated PDMS, while the latter is a mixture of dimethylsiloxane and a platinum complex and copolymers of methylhydrosiloxane. Through a hydrosilylation reaction between vinyl and hydrosilane groups, the mixture of the two components becomes a cross-linked solid elastomer after a few hours of curing time [20, 21].

The patterned NFG film was held flat in a Petri dish and the precursor solution mixed with curing agent (10:1 ratio) was gently poured on top to fill the BF-generated holes and produce a uniform 4–5 mm thickness backing layer for ease of subsequent handling. The solution was

then left to cure for 48 h at room temperature, a protocol designed to maximize the fidelity of the elastomeric replica. After curing, the PDMS BF replica and backing layer could easily be separated from the patterned NFG film. The PDMS master was then washed thoroughly with dichlorobenzene or another suitable solvent to ensure that there was no possibility for cross-contamination (transfer of NFG residues) during subsequent printing. An AFM image ( $25 \times 25 \mu\text{m}^2$ ) of a typical PDMS replica is shown in figure 1(b). The fidelity of the replica is excellent: the observed defects shown in this image replicate defects in the original BF pattern formed in the NFG film.

### 3. Fabrication of micro-structured F8BT/TFB polymer blend LEDs

To fabricate micro-structured LEDs, ITO-coated glass substrates were washed thoroughly using detergent and subsequently rinsed with water, acetone and isopropanol. After washing, the ITO-coated substrates were dried on a hot plate at  $100^\circ\text{C}$  for about 10 min. They were then plasma etched for 1 min at 100 W and poly(3,4-ethylenedioxythiophene)/polystyrenesulphonic acid (PEDOT:PSS) from HC Starck (Baytron P Al 4083) was spin coated on them immediately afterwards. Plasma treatment of the ITO layer has been demonstrated to improve the injection performance of the anode [22, 23]. The samples were then left on the hotplate at  $140^\circ\text{C}$  for 1 h to harden the PEDOT:PSS layer. The devices which were to be patterned were then taken to a spin coater where a  $30 \text{ g l}^{-1}$  solution of polyimide (PI) precursor (30 mg of Merck Liquicoat PI-Resin dissolved in 1 ml of Merck Liquicoat Thinner) was deposited at a spin speed of 1000 rpm, resulting in a 130 nm thickness film. Solvent-assisted micro-moulding, as described by Xia *et al* [21], was next used to pattern an array of holes right through the PI precursor layer to the underlying PEDOT:PSS/ITO-coated substrate. The much greater height ( $\approx 800 \text{ nm}$ ) of the PDMS replica features than the PI precursor film thickness ( $\approx 130 \text{ nm}$ ) helps to facilitate this. The PDMS replica was inked with Merck Liquicoat Thinner, lightly hand-pressed against the PI precursor film and held in place until the solvent had evaporated. On removal of the PDMS replica, the glass/ITO/PEDOT:PSS/patterned film structures were placed on a hot plate overnight at  $75^\circ\text{C}$  to imidize the PI precursor. A schematic diagram of the patterning process for the PI layer is depicted in figure 2.

The resulting BF patterned PI film (see optical micrograph in figure 1(c) ( $75 \times 75 \mu\text{m}^2$ )) is highly insulating and insoluble in common organic solvents, properties that allow an emissive polymer layer to be spin coated on top (see optical micrograph in figure 1(d) ( $75 \times 75 \mu\text{m}^2$ )) and make electrical contact to the ITO anode via the PEDOT:PSS layer only within those areas corresponding to BF holes. The patterned PI film thus defines the active areas for multiple, micron-sized, polymer blend LEDs. In this way its use is similar to the bank structures used to define the pixels in state-of-the-art ink jet printed polymer electroluminescent (EL) displays [24], or in developmental contact printed displays [25]. Here, however, as a first demonstration of the method, we simply blanket cover the pattern rather than selectively deposit different emission colour materials at different locations as would be required for a colour display. PI has other desirable properties for this application, namely it has no discernible absorption or fluorescence in the visible spectral range and it causes no appreciable change in the luminescent properties of subsequently deposited polyfluorenes [26, 27], the polymer class we have used as the emissive materials in our LEDs. The defects and domains observed in figure 1(c) are a faithful replica of the original BF film. It is then understood that better control of the BF formation mechanism and/or selection of the area chosen to make the replica stamp will significantly improve the regularity of the final hexagonal array.

To try and make sure that any PI residue that might be present at the bottom of the printed holes is removed, the devices were treated again with the plasma asher for 2 min at

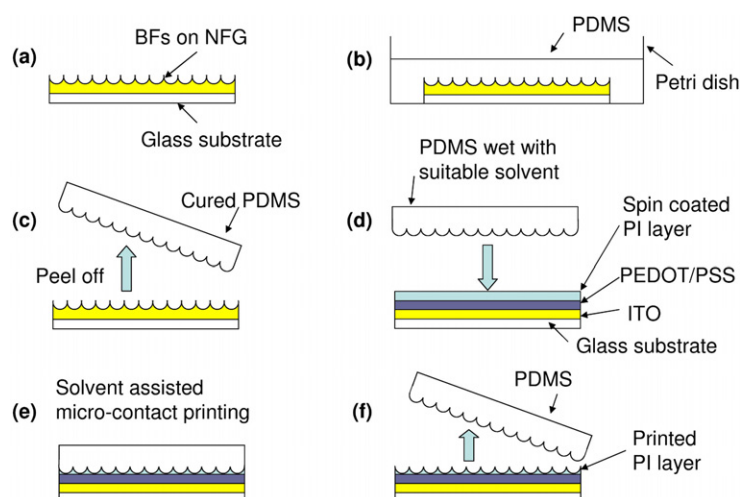


**Figure 2.** (a) Breath figures are formed in an NFG polymer layer on a glass substrate. (b) The substrate is then placed in a Petri dish and covered with PDMS. (c) Once the PDMS has cured, the elastomer stamp is separated from the original BF film and trimmed to size. (d) After wetting with a suitable solvent the stamp is brought into contact with the PI layer spin coated on top of a PEDOT:PSS film on an ITO-coated glass substrate. (e) The PDMS master is pressed into the PI layer and the solvent is allowed to evaporate. (f) The PDMS master is finally removed to leave behind the PI layer patterned with a replica of the BF structure.

(This figure is in colour only in the electronic version)

20 W. The low power used ensured that the rest of the PI was not significantly affected by the treatment. Moreover, a control device was made to ensure that the possible accidental plasma treatment of the PEDOT:PSS layer after removal of the PI would not damage the device: a PEDOT:PSS-coated ITO layer on a glass substrate was plasma treated at 20 W for 2 min prior to emissive layer deposition and no negative changes in the device performance could be detected. After plasma treating the PI, the emission layer was spin coated at 2500 rpm on top of either the patterned PI or the PEDOT:PSS layer (for samples with no pattern) from a  $18 \text{ g l}^{-1}$  xylene solution of poly(9,9-dioctylfluorene-*co*-benzothiadiazole) (F8BT) and poly(9,9-dioctylfluorene-*co*-*N*-(4-butylphenyl) diphenylamine) (TFB) in a 1:1 weight ratio. When spin coated on a flat substrate under the same conditions, the active layer formed is  $\approx 90 \text{ nm}$  in thickness. A profilometer measurement on the patterned area after the active layer had been spin coated revealed a surface roughness of about 40–50 nm. Figure 1(d) shows an optical micrograph ( $75 \times 75 \mu\text{m}^2$ ) of such a sample. The non-uniformity in the colour of this image is probably the result of phase separation between the two polymers of the active blend: F8BT and TFB are indeed known to phase separate when spin coated from xylene solution [28]. This tendency to spatial variations in blend composition has been shown to be desirable, resulting as it does in enhanced device performance [29]. Finally, a common cathode, consisting of  $\approx 1 \text{ nm}$  thickness of LiF and  $\approx 100 \text{ nm}$  thickness of Al, was evaporated on top of the F8BT/TFB blend film using a shadow mask to define an active area of  $4 \text{ mm}^2$  (the overlap between the two electrodes).

#### 4. Characterization of micro-structured polymer blend LED performance

The resulting F8BT/TFB blend LEDs were tested under a nitrogen atmosphere to avoid short-term degradation: current density ( $J$ ) versus voltage ( $V$ ) characteristics were measured with a

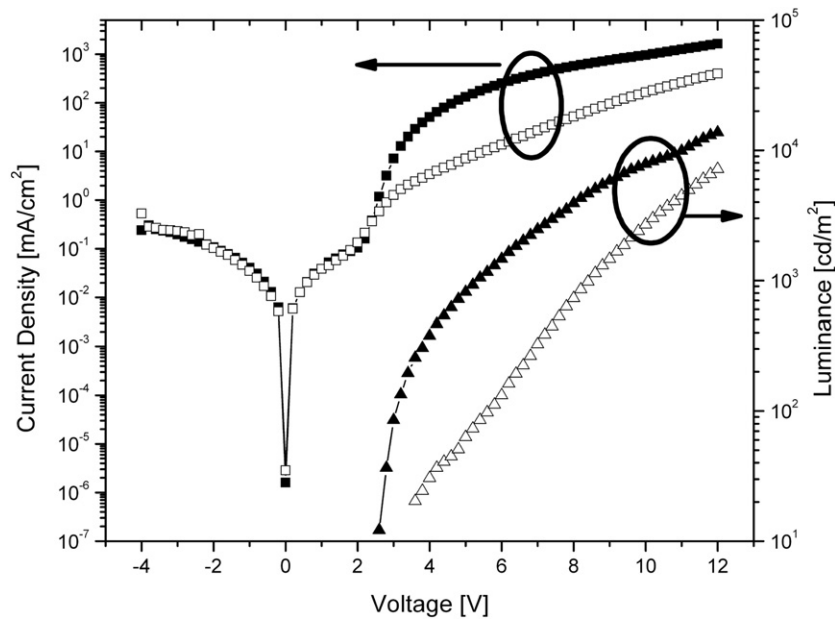


**Figure 3.**  $J$ - $V$ - $L$  characteristics of normal (filled data symbol) and micro-structured (empty data symbols) LEDs: the current density,  $J$ , data are shown by squares and the luminance,  $L$ , data by triangles.

Keithley 2400 voltage source/current meter and the device luminance ( $L$ ) was simultaneously monitored with a TOPCON BM-9 luminance meter. An optical fibre bundle fed spectrometer comprising a spectrograph and charge-coupled device (CCD) detector was used to measure the EL spectrum. The  $J$ - $V$ - $L$  characteristics of typical devices with and without the BF-derived structure are presented in figure 3: the luminance typically reaches  $L \approx 7200 \text{ cd m}^{-2}$  at a current density  $J \approx 450 \text{ mA cm}^{-2}$  for  $V = 12 \text{ V}$  for patterned devices while non-patterned devices reach  $L \approx 13700 \text{ cd m}^{-2}$  and  $J \approx 1630 \text{ mA cm}^{-2}$  for the same applied voltage. These data have been corrected to take into account the fact that the current flow and EL emission are heterogeneous, and specifically that the area occupied by the apertures in the PI film is only  $\approx 60\% \pm 10\%$  of the total area. This was estimated by imaging a patterned area of the sample and calculating the relative space occupied by the BF holes. The lower current density and slightly higher turn-on voltage for patterned LEDs is probably to be ascribed to the fact that patterned devices tend to be on average thicker than non-patterned ones, an effect that was also seen in our earlier study on small-area LEDs [11]. There the drive voltage for  $100 \text{ cd m}^{-2}$  luminance increased from 5 V for unpatterned LEDs to 12 V for  $50 \mu\text{m}$  diameter structures (defined by lithographically patterning holes in a silicon nitride overlayer on the ITO-coated glass substrate).

The device current ( $\text{cd A}^{-1}$ ) and power ( $\text{lm W}^{-1}$ ) (inset) efficiencies are shown in figure 4: for non-structured devices the current and power efficiencies peak at about 3 V ( $1.2 \text{ cd A}^{-1}$  and  $1.28 \text{ lm W}^{-1}$ ) and then rapidly decrease with increasing voltage. In contrast the current efficiency for patterned devices shows a gradual increase across the measured voltage range and is always higher (after turn-on) than for normal devices. In particular, at 12 V, the micro-LEDs show both current and power efficiencies that are twice as large as those for non-patterned devices. Moreover, the micro-LED power efficiency remains pretty much constant across the measured voltage range, providing a relatively stable performance. This behaviour contrasts

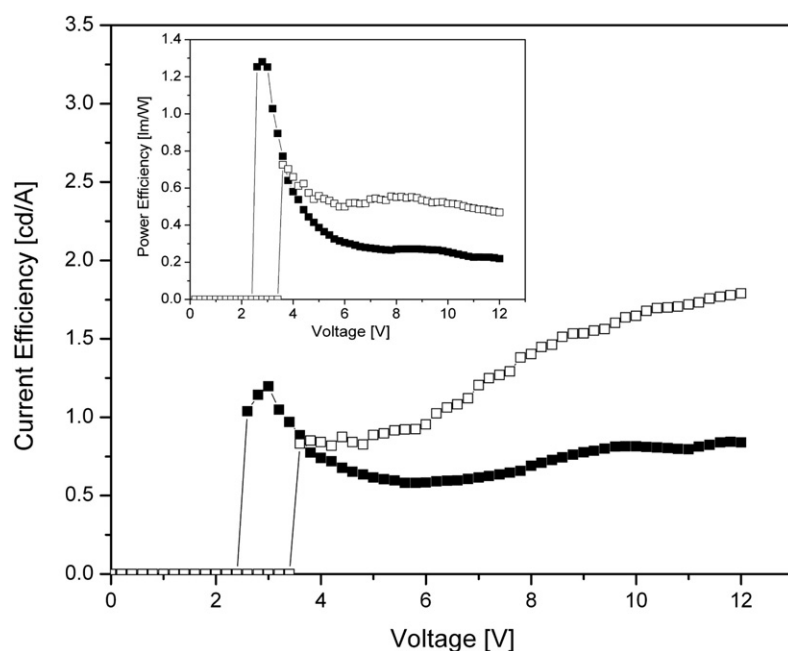


**Figure 4.** Current and power efficiency (inset) of normal (filled data points) and micro-structured (empty data points) LEDs.

with that seen for our previously reported small-area polymer LEDs [11], where the smallest ( $50\ \mu\text{m}$  diameter) structures had a reduced efficiency relative to unpatterned structures.

The improved efficiency of our patterned devices could be the result of a combination of several factors: these include process/device structure-related changes in electrical characteristics, the better thermal management within small-area LEDs [11, 19], and the effects of light scattering introduced by the printed structure [8–10]. The latter is expected to help to reduce in-plane waveguiding of the emitted light, one of the major causes for light loss in LEDs [30, 31], and should thus improve the desirable light output normal to the device plane [9, 10]. Separating the contributory factors to the improved efficiency is difficult for our devices given the already noted changes in film thickness and blend morphology that accompany the fabrication of these micron-scale LEDs. Adawi *et al* [10] recently reported red-emitting polymer LED structures in which a silicon nitride layer was patterned as a 2D square array of  $\approx 1\ \mu\text{m}$  diameter/450 nm in height pillars (on a  $1.2\ \mu\text{m}$  pitch), infilled and planarized with a spin-on glass and coated with ITO to act as a scattering substrate. This procedure allowed a direct comparison of structures with identical electrical performance (fabrication of the LED on a standard ITO-coated glass substrate or one of these scattering substrates does not affect its electrical performance) and showed that the scattering substrate LEDs had a two-fold enhanced efficiency, albeit at rather low levels of overall device performance ( $0.1\ \text{cd A}^{-1}$  efficiency at  $100\ \text{cd m}^{-2}$  luminance at 10 V for the standard substrate devices).

Figure 5 shows the normalized EL spectra (measured at  $100\ \text{cd m}^{-2}$ ) for a micro-structured LED (open circles) and for a standard LED (filled squares) fabricated using the same F8BT/TFB blend solution and with the same electrode deposition steps. Neither was found to depend on bias voltage across the range 6–20 V. The EL spectrum of the micro-structured LED is very slightly red-shifted and marginally less structured with respect to that



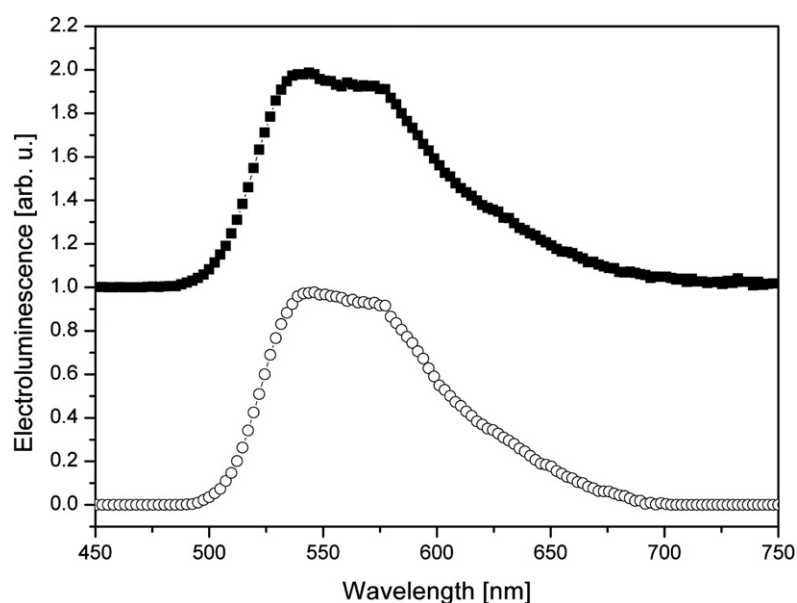


**Figure 5.** Normalized electroluminescence spectra (both measured at  $100 \text{ cd m}^{-2}$ ) for a microstructured polymer blend LED (open circles) and a standard (non-patterned) polymer blend LED (filled squares). The latter spectrum is displaced vertically for clarity.

of the non-patterned LED, leading to very modest changes in the Commission Internationale de l'Eclairage (CIE) 1931(X, Y) colour coordinates from (0.43, 0.55) to (0.43, 0.56). More detailed studies will be required to fully determine the origin of this effect.

## 5. Summary and conclusion

In summary, we have demonstrated the use of BF pattern formation in a polymer thin film as a means to produce PDMS masters possessing arrays of micron-size protrusions that can subsequently be used to pattern the active layer of organic thin-film device structures. By way of illustration, we used such a stamp to pattern an insulating PI layer on top of a PEDOT:PSS covered ITO-coated glass substrate, thus defining an array of micro-receptacles. Plasma etching was used to ensure the removal of possible residual PI at the bottom of the holes. These were filled by spin coating an F8BT/TFB blend solution on top and a LiF/Al cathode was then evaporated onto the resulting blend film to fabricate an array of micro-LEDs. The devices thus produced show higher current and power efficiency than non-patterned devices. The fabrication approach further benefits from the ability to simply tune the features of the master by varying the conditions under which the BF patterns are formed. The method introduced in this paper appears to have significant potential for organic device fabrication.

## Acknowledgments

The authors thank Rob Fletcher, Mike Inbasekaran and Jim O'Brien of The Dow Chemical Company for providing the NFG, F8BT and TFB copolymers that were used in these experiments. We also thank the UK Engineering and Physical Sciences Research Council for funding this work (Ultrafast Photonics Collaboration IRC GR/R55078 and GR/R26641). Finally, we thank Dr Mohan Srinivasarao for useful discussions on BF formation procedures.

## References

- [1] Aitken J 1892 *Proc. R. Soc. Edinburgh* **20** 94–7  
Aitken J 1911 *Nature* **86** 516  
Lord Rayleigh 1911 *Nature* **86** 416  
Lord Rayleigh 1912 *Nature* **90** 436  
Aitken J 1913 *Nature* **90** 619
- [2] Beysen D and Knobler C M 1986 *Phys. Rev. Lett.* **57** 1433–6  
Steyer A, Guenoun P, Beysen D and Knobler C M 1990 *Phys. Rev. B* **42** 1086–9
- [3] Widawski G, Rawiso M and Francois B 1994 *Nature* **369** 387–9
- [4] Srinivasarao M, Collings D, Philips A and Patel S 2001 *Science* **292** 79–83
- [5] Peng J, Han Y, Yang Y and Li B 2004 *Polymer* **45** 447–52
- [6] Erdogan B, Song L, Wilson J N, Park J O, Srinivasarao M and Bunz U H F 2004 *J. Am. Chem. Soc.* **126** 3678–9
- [7] Haupt M, Miller S, Sauer R, Thonke K, Mourran A and Moeller M 2004 *J. Appl. Phys.* **96** 3065–9
- [8] Lawrence J R, Andrew P, Barnes W L, Buck M, Turnbull G A and Samuel I D W 2002 *Appl. Phys. Lett.* **81** 1955–7
- [9] Corcoran N, Ho P K H, Arias A C, MacKenzie J D, Friend R H, Fichet G and Huck W T S 2004 *Appl. Phys. Lett.* **85** 2965–7
- [10] Adawi A M, Kullock R, Turner J L, Vasilev C, Lidzey D G, Tahraoui A, Fry P W, Gibson D, Smith E, Foden C, Roberts M, Qureshi F and Athanassopoulou N 2006 *Org. Electr.* **7** 222–8
- [11] Wilkinson C I, Lidzey D G, Palilis L C, Fletcher R B, Martin S J, Wang X H and Bradley D D C 2001 *Appl. Phys. Lett.* **79** 171–3
- [12] Beh W S, Kim I T, Qin D, Xia Y N and Whitesides G M 1999 *Adv. Mater.* **11** 1038–41
- [13] Sun Y R, Shtein M and Forrest S R 2005 *Appl. Phys. Lett.* **86** 113504
- [14] Wei M K and Su I L 2004 *Opt. Express* **12** 5777–82
- [15] Bolognesi A, Mercogliano C, Yunus S, Civardi M, Comoretto D and Turturro A 2005 *Langmuir* **21** 3480–5
- [16] Shkunov M N, Vardeny Z V, Delong M C, Polson R C, Zakhidov A A and Baughman R H 2002 *Adv. Funct. Mater.* **12** 21–6
- [17] Tai C Y, Unal B, Wilkinson J S, Ghanem M A and Bartlett P N 2004 *Appl. Phys. Lett.* **84** 3513–5
- [18] Fichet G, Corcoran N, Ho P K H, Arias A C, MacKenzie J D, Huck W T S and Friend R H 2004 *Adv. Mater.* **16** 1908–12
- [19] Boroumand F A, Hammiche A, Hill G and Lidzey D G 2004 *Adv. Mater.* **16** 252–5
- [20] Clarson S J and Semlyen J A 1993 *Siloxane Polymers* (Englewood Cliffs, NJ: Prentice-Hall)
- [21] Xia Y N and Whitesides G M 1998 *Annu. Rev. Mater. Sci.* **28** 153–84
- [22] Wu C C, Wu C I, Sturm J C and Kahn A 1997 *Appl. Phys. Lett.* **70** 1348–50
- [23] Kim J S, Cacialli F and Friend R H 2003 *Thin Solid Films* **445** 358–66
- [24] Lee D, Chung J R, Wang J, Hong S, Choi B, Cha S, Kim N, Chung K, Gregory H, Lyon P, Creighton C, Carter J, Hatcher M, Bassett O, Richardson M and Jerram P 2005 *Conf. Proc. SID 05, DIGEST* 527–29
- [25] Nakajima H, Morito S, Nakajima H, Takeda T, Kadowaki M, Kuba K, Handa S and Aoki D 2005 *Conf. Proc. SID 05, DIGEST* 1196–99
- [26] Heliotis G, Xia R, Whitehead K S, Turnbull G A, Samuel I D W and Bradley D D C 2003 *Synth. Met.* **139** 727–30
- [27] Xia R, Campoy-Quiles M, Heliotis G, Stavrinou P, Whitehead K S and Bradley D D C 2005 *Synth. Met.* **155** 274–8
- [28] Kim J S, Ho P K H, Murphy C E and Friend R H 2004 *Macromolecules* **37** 2861–71
- [29] Morteani A C, Dhoot A S, Kim J S, Silva C, Greenham N C, Murphy C, Moons E, Cina S, Burroughes J H and Friend R H 2003 *Adv. Mater.* **15** 1708–12
- [30] Ziebarth J M, Saafir A K, Fan S and McGehee M D 2004 *Adv. Funct. Mater.* **14** 451–6
- [31] Sims M, Zheng K, Campoy-Quiles M, Xia R, Stavrinou P N, Bradley D D C and Etchegoin P 2005 *J. Phys.: Condens. Matter* **17** 6307–18